Wireless Netw (2014) 20:2503–2519
DOI 10.1007/s11276-014-0752-8

Performance analysis of greedy fast-shift block acknowledgement for high-throughput WLANs

Wen-Jiunn Liu · Chao-Hua Huang · Kai-Ten Feng · Po-Hsuan Tseng

Published online: 18 June 2014

Abstract The techniques of frame aggregation and block acknowledgement (ACK) are utilized in the IEEE 802.11n standard for achieving high throughput performance from the medium access control perspective. Conventional greedy scheme for block ACK adopts the transmitter-defined starting sequence number (SSN) to construct the ACK window for recognizing the correctness of data packets. However, there exists correctly received packets that lie outside of the ACK window which will unavoidably be retransmitted by adopting the conventional scheme. In this paper, a greedy fast-shift (GFS) block ACK mechanism is proposed to provide the receiver-defined SSN, which can both implicitly acknowledge the correctly received packets before the SSN and explicitly identify the correctness information for the packets after the SSN. In order to evaluate the effectiveness of the GFS scheme, the analytical models for these two mechanisms are proposed based on the window utilization. Compared to the conventional greedy scheme, it is observed from the simulation results that the proposed GFS method can provide better performance owing to its fast-shift behavior on ACK window.

W.-J. Liu · C.-H. Huang · K.-T. Feng (✉)
Department of Electrical and Computer Engineering, National Chiao Tung University, Hsinchu, Taiwan
e-mail: ktfeng@mail.nctu.edu.tw

W.-J. Liu
e-mail: jiunn.cm94g@nctu.edu.tw

C.-H. Huang
e-mail: chhuang.cm98g@nctu.edu.tw

P.-H. Tseng
Department of Electronic Engineering, National Taipei University of Technology, Taipei, Taiwan
e-mail: phtseng@ntut.edu.tw

Keywords Wireless local area network · IEEE 802.11n · Medium access control · Block acknowledgement

1 Introduction

A wireless network is a type of computer networks that utilizes wireless communication technologies to maintain connectivity and exchange messages. Depending on the size of wireless coverage, the IEEE standards association establishes five standard series to enable wireless transmission. Among these wireless standard series, the IEEE 802.11 standard designed for wireless local area networks (WLANs) is considered the well-adopted suite for indoor, high speed communication due to its remarkable success in both design and deployment.

Various amendments are contained in the IEEE 802.11 standard suite, mainly including IEEE 802.11a/b/g [1–3], IEEE 802.11e [4] for quality-of-service (QoS) support, and IEEE 802.11n [5] for high throughput performance. In order to fulfill the requirement for achieving enhanced throughput, the IEEE 802.11 Task Group N (TGn) enhances the the physical layer (PHY) data rate by adopting advanced communication techniques, such as orthogonal frequency-division multiplexing (OFDM) [6] and multi-input multi-output (MIMO) [7] technologies. However, it has been investigated in [8] that simply improves the PHY data rate will not suffice for enhancing the system throughput from the medium access control (MAC) perspective. Accordingly, the IEEE 802.11 TGn further exploits packet aggregation techniques to moderate the drawbacks that are originated form the MAC/PHY overheads.

There are research works proposed in [9–18] that focus on the schemes for data packet aggregation. Xiao [9] has

suggested to adopt packing, concatenation, and multiple frame transmission in order to reduce the MAC/PHY overheads. Lu et al. [10] recommended the MAC queue aggregation (MQA) scheme for the enhancement of VoIP traffic; while Wu [11] proposed the differentiated data aggregation (DDA) mechanism which exploited the multilevel modulation from the PHY layer for improving the data aggregation of the WLANs. Ghazisaidi et al. [12] further considers the joint aggregation effects with the Ethernet passive optical network (EPON) [19] system in the hybrid optical fiber-wireless (FiWi) broadband access networks [20]. It is also noted that two-level aggregation techniques, i.e., the aggregate MAC service data unit (A-MSDU) and the aggregate MAC protocol data unit (A-MPDU), are adopted within the IEEE 802.11n standard for performance enhancement of the network throughput. The performance of the A-MSDU and A-MPDU schemes has been analyzed in the research works [21–24], and the decision of the optimal frame size can be found in [25]. Finally, the implementation and experiments are conducted in [26] for validating the effectiveness of the frame aggregation schemes.

It has been studied that the large amount of small-sized control packets, i.e., the acknowledgement (ACK) packets, can significantly degrade the throughput performance [27]. The use of the stop-and-wait automatic repeat request (ARQ) [28] in the prior wireless LAN standard takes the major blame for the creation of these small ACK packets since each data packet should be acknowledged by an independent ACK packet. Due to the observed inefficiency, the block ACK mechanism has been specified in both the IEEE 802.11e and IEEE 802.11n standards for the aggregation of ACK packets. It is noted that the block ACK scheme utilizes comparably longer payload to accommodate the information from numerous ACK packets, which can effectively reduce the total number of required ACK packets. The IEEE 802.11 standard provides the message format to support multiple ACK packets. However, the algorithm to perform block ACK is not specified in the standard and it should be designed to match the message format.

Based on the IEEE 802.11e and IEEE 802.11n standard, several block ACK algorithms are proposed to accommodate larger size of ACK aggregation. One of the representative block ACK schemes is the extended block ACK (EBA) mechanism [29, 30]. In order to distinguish from the proposed scheme, the EBA mechanism is denoted as the conventional greedy scheme (GS) in this paper. Initially, the transmitter assigns each packet with a specific sequence number. Based on these sequence numbers, the receiver initiates the block ACK packet which contains the bitmap with its first bit beginning from a specific starting sequence number (SSN). The transmitter will be informed regarding the correctness of each numbered packet, i.e., the ACK window ranging from the SSN to the end sequence number of the bitmap. Afterwards, the GS scheme will resend the unsuccessfully received packets together with the new-coming packets in order to both recover the packet errors and enhance the system throughput. However, the limited bitmap size may cause the problem that some correctly received data packets can not be properly acknowledged since these packets may lie outside of the ACK window defined by the SSN value. In the conventional GS scheme, significant throughput degradation due to this problem can be frequently observed since the transmitter is in charge of determining the SSN value. It therefore lacks the flexibility of changing the SSN value since more information can be obtained from the receiver side. The details of the GS scheme and its underlying problem will further be described in the next section.

In this paper, a greedy fast-shift (GFS) block ACK mechanism is proposed from the receiver's point of view to reduce the occurrence of the aforementioned problem due to the insufficient bitmap size. Based on the proposed GFS scheme, the receiver will derive and provide the SSN value which carries additional information that the packet with sequence number (SN) smaller than the SSN are considered correctly received. It can both implicitly acknowledge the correctly received packets before the SSN and also explicitly provide the correctness information for the packets after the SSN. The SSN value can therefore be increased faster than the conventional GS scheme, which effectively mitigates the performance degradation resulting from the insufficient bitmap. Furthermore, analytical models for these two block ACK mechanisms are proposed based on the Markov chain techniques [31] to evaluate the window utilization from the mathematical point of view. The correctness and effectiveness of the derived analytical models are validated via simulations. With respect to system throughput, end-to-end delay, and blocking overhead, it is observed from the simulation results that the proposed GFS scheme outperforms the conventional GS method under different packet error probabilities and window sizes.

The rest of this paper is organized as follows. Section 2 describes both the conventional GS scheme and the GFS ACK mechanism. The proposed analytical models for both schemes are further derived and explained in Sect. 3. Section 4 shows the performance validation and comparison of these two schemes via simulations. Section 5 draws the conclusions.

2 Block acknowledgement mechanisms

In this section, the conventional GS scheme and its underlying problem will first be described. Furthermore,

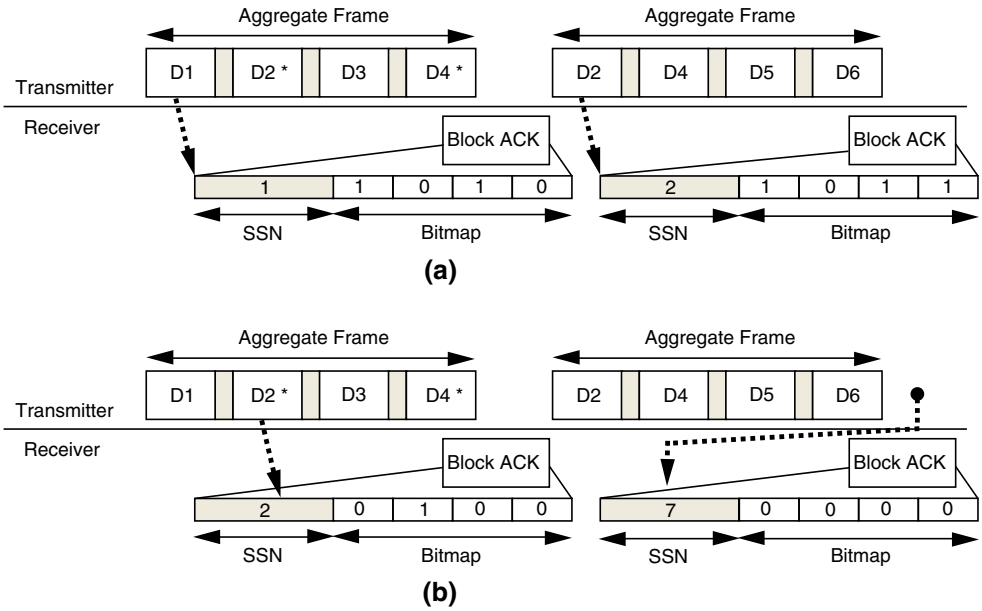

Fig. 1 Examples for the two block ACK mechanisms under window size $W = 4$: **a** the conventional greedy scheme (GS), and **b** the proposed greedy fast-shift (GFS) scheme

the proposed GFS mechanism for block ACK will be explained as follows.

2.1 Conventional greedy scheme

The conventional block ACK mechanism denoted as the GS scheme is described in this subsection. For the generalization of data aggregation mechanisms, a system parameter called window size W is introduced to denote the maximum number of data packets that are contained within a single frame. The characteristics of the conventional GS scheme is explained with the example as shown in Fig. 1(a) under $W = 4$ as follows.

In the conventional GS scheme, the transmitter assigns each data packet with an SN for packet identification, e.g., SN $= 1$ for D1 and SN $= 2$ for D2. As illustrated in Fig. 1(a), the first aggregate frame consisting of W data packets from D1 to D4 is delivered by the transmitter; while both D2 and D4 packets denoted with the $*$ sign are considered corrupted. The block ACK packet consists of an additional SSN field in front of its bitmap array to record the sequence number of the starting packet within the aggregate frame, e.g., SSN $= 1$ denotes that D1 is the starting packet in the first frame; and SSN $= 2$ represents D2 as the starting packet for the second frame. Moreover, the bitmap array of size W within the block ACK packet indicates the packet correctness based on the consecutive SNs.

As shown in Fig. 1(a), the bitmap from the first block ACK packet $b = [1010]$ with SSN $= 1$ contains the correctness information of the aggregated data packets from SN $= 1$ to SN $= 1 + (W - 1) = 4$, i.e., for the consecutive D1 to D4 data packets. It is noticed that the one value within the bitmap denotes that the corresponding packet is correctly received; while the zero value implies that the correctness of the corresponding packet should be determined by the transmitter since the packet can be either corrupted or previously acknowledged. After the reception of the first block ACK packet, the transmitter redelivers the previously unacknowledged D2 and D4 packets together with the newly scheduled D5 and D6 packets in the second aggregate frame. Associated with SSN $= 2$ and bitmap $b = [1011]$ in the second block ACK packet, the receiver notifies the transmitter that D2, D4, and D5 packets are correctly received while the correctness of D3 packet is undetermined. Based on the previous reception within the transmitter, it can be observed that packet D3 was successfully received such that it is not required to be retransmitted. Furthermore, it is worthwhile to notice that the correctness of packet D6 becomes undetermined even though it is correctly received by the receiver. The performance degradation due to the insufficient bitmap for recording the correctness information can therefore be perceived.

2.2 Proposed greedy fast-shift (GFS) scheme

The GFS block ACK mechanism is proposed in this subsection as an enhanced version of the conventional GS scheme. The main objective of the proposed GFS scheme is to mitigate the performance degradation due to insufficient bitmap of the conventional GS scheme. The procedures of proposed GFS scheme with $W = 4$ is illustrated in the exemplified schematic diagram of Fig. 1(b). Inherited from the conventional GS scheme, the characteristics of both the SN and SSN fields in the

transmitter side are still preserved. For efficiency consideration, the mechanism of retransmitting both the corrupted packets and the new-coming packets are also employed. The major differences between the proposed GFS mechanism and the conventional GS scheme are on the methodologies to determine the SSN value at the receiver side. In the GS scheme, the SSN of the feedback block ACK packet is determined by the SN of first packet in the aggregate frame. In other words, the receiver does not change the value of SSN, which is actually assigned by the transmitter. On the other hand, in the proposed GFS scheme, the SSN value is given by the receiver as the SN of the first unreceived data packet. Consequently, the SSN value of the block ACK packet may not necessarily be equal to the SN of first packet in the aggregate frame. It can be a larger value or even beyond the largest SN in the aggregate frame.

The bitmap array, i.e., the ACK window, specified in the block ACK packet of the proposed GFS scheme still represents the packet correctness based on the consecutive SNs starting with the SSN value. Consider the same case as in Fig. 1(a), the packets D2 and D4 in the first aggregate frame of Fig. 1(b) are corrupted. Instead of receiving the block ACK with SSN = 1, the transmitter receives a block ACK packet with SSN = 2 in the proposed GFS scheme since the SSN is determined by the receiver as the SN of the first unreceived data packet, i.e., the packet D2. Likewise, after the reception of the first block ACK packet, the transmitter redelivers the previously unacknowledged D2 and D4 packets together with the newly scheduled D5 and D6 packets in the second aggregate frame. After receiving the second aggregate frame with correct D2, D4, D5, and D6 packets, the receiver knows that the data packets from D1 to D6 are correctly received. Therefore, the receiver assigns the SSN to be 7 which is the SN of the first unreceived packets. It can be observe that the SSN value will be larger than the SN's range of the aggregate frame. Afterwards, the receiver sends the block ACK packet with SSN = 7 and bitmap $b = [0000]$, which indicates that the receiver does not receive packets from D7 to D10 and all the packets before D7, i.e., D1 to D6, are correctly received.

Instead of providing explicit ACK to each packet in the aggregate frame, the proposed GFS scheme adopts a hybrid method to both implicitly acknowledge the correctly received packets before the SSN and also explicitly provide the correctness information of those packets after the SSN. Contributing to this hybrid method, the SSN value will grow faster than that in the conventional GS scheme, resulting in the phenomenon of fast-shift ACK window specified in the block ACK packet. The performance degradation due to the insufficient bitmap can therefore be mitigated. The detailed processes and the analytical model of the proposed GFS scheme are further explained in Sect. 3.2.

3 Proposed Markovian chain-based analytical models for block acknowledgement mechanisms

In this section, two proposed analytical models for the conventional GS scheme and the proposed GFS mechanism will be respectively formulated based on the Markov chain techniques. The main target of both analytical models is focused on the throughput performance based on the metrics of window utilization. The window utilization is defined as the average number of successfully acknowledged packets within an aggregate frame divided by the window size W. It is intuitive to directly relate the window utilization to the system throughput of the corresponding scheme. In order to simplify the derivations of the proposed analytical models, one transmitter/receiver pair for packet transmission is considered in the network. Moreover, it is assumed that all data packets possess the same packet error probability p_e; while the block ACK packets are considered correctly received. The explanation of the two proposed analytical models are stated as follows.

3.1 Analytical model for conventional greedy scheme

The analytical model for the conventional GS scheme is constructed by adopting the Markov chain techniques. Based on the Markovian approach, there exists a state transition diagram consisting of internal states and the respective state transition probability. In this subsection, the internal states for the analytical model of the GS scheme will first be defined. The underlying state transition diagram with the transition probability for the corresponding state transition is also properly formulated. Finally, the derivation of window utilization for the GS scheme concludes the analytical model. It is noted that all the context will be provided based on the generic analytical model with window size W. An illustrative example under $W = 3$ will be addressed for further explanation.

3.1.1 Internal states

In order to define the internal states of GS scheme, three parameters are first introduced, including the transmitter correctness bitmap, the middle union, and the state index. The transmitter correctness bitmap represents the Boolean correctness array for all numbered data packets from the transmitter's perspective. The state index is a set of W binary digits with its most significant bit located at the first zero of the transmitter correctness bitmap. The middle union is acquired by implementing the bitwise OR

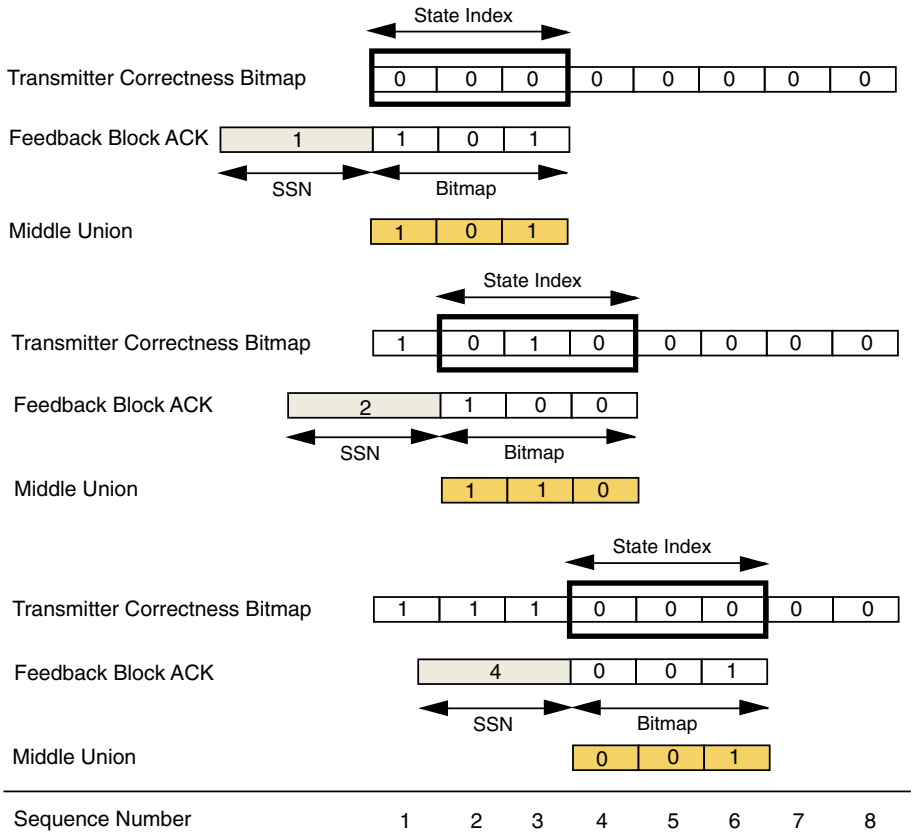

Fig. 2 The three critical parameters for the internal state definition of the conventional GS scheme: the transmitter correctness bitmap, the middle union, and the state index

operation on the current state index and the feedback block ACK bitmap. It is also noted that the state index will be utilized to define its respective internal state.

The illustrative example for the three critical parameters under the window size $W = 3$ is shown in Fig. 2. Initially, the transmitter correctness bitmap is an all-zero array, which results in the state index $k = [000]$. The transmitter starts to deliver the numbered data packets D1, D2, and D3 to the receiver. It is assumed that a feedback block ACK packet with a bitmap of $b = [101]$ is consequently acquired by the transmitter. As a result, the middle union can be computed as $m = k \cup b = [000] \cup [101] = [101]$. As illustrated in Fig. 2, the transmitter correctness bitmap is also updated by recording the bit values in the middle union into its corresponding bits. As the transmitter correctness bitmap is changed, the state index is consequently shifted to become $k = [010]$ based on its definition. According to the conventional GS scheme, the transmitter redelivers the previously corrupted packet D2 together with the newly scheduled packets D4 and D5, and receives a feedback block ACK packet consisting of a bitmap $b = [100]$. As a consequence, the new state index will be calculated and obtained as $k = [000]$ as in Fig. 2.

Based on the definition, the state index must have the leading zero to represent either a previously corrupted or a newly scheduled packet. Therefore, the conventional GS

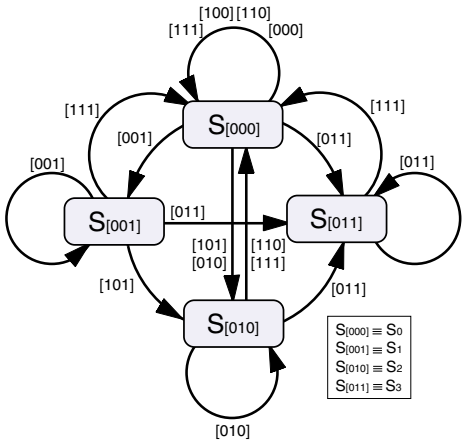

Fig. 3 State transition diagram for the conventional GS scheme under the window size $W = 3$: each state transition is represented as a unidirectional link with the causal middle union of width W

scheme will possess a total of 2^{W-1} internal states that are denoted as S_k with the state index $k \in [0, 1, ..., (2^{W-1} - 1)]$. As shown in Fig. 3, four states S_0 to S_3 exist in the state transition diagram for the conventional GS scheme under the window size $W = 3$. In order to facilitate the explanation, each state can be represented by either the decimal

or the binary subscript, i.e. $S_0 \equiv S_{[000]}, S_1 \equiv S_{[001]}, S_2 \equiv S_{[010]}$, and $S_3 \equiv S_{[011]}$.

3.1.2 State transition diagram

In the state transition diagram of window size W, there exist 2^{W-1} internal states and their corresponding state transitions. Each transition between two states is represented as a unidirectional link from the original state S_i to the resulting state S_k. Moreover, the potential middle unions that result in the state transition are also shown around the link. The representative state transition diagram under the window size $W = 3$ is illustrated in Fig. 3. Consider that the transition from $S_{[001]}$ to $S_{[010]}$ is resulted from the middle union $m = [101]$, the middle union $m = [101]$ will consequently let the transmitter increase the SSN by one, causing the state index to become $k = [010]$, i.e. the state of $S_{[010]}$. It is noted that the mechanism for acquiring the resulting state can be generalized by the rule as to remove all the leading ones in the middle union and pad an equal number of zeros from the right-hand side.

3.1.3 State transition probability

As shown in Fig. 3, the state transition probability from $S_{[001]}$ to $S_{[010]}$ can be computed from the bit values within the middle union $m = [101]$ as $G_{[001]\to[010]} = (1 - p_e) \cdot p_e$, where p_e denotes the packet error probability and $G_{[001]\to[010]}$ represents the transition gain from $S_{[001]}$ to $S_{[010]}$. It is noticed that the rightmost bit within the middle union is not considered in the computation of packet error probability since the data packet was correctly received in the previous transmission. The generic transition probability from S_i to S_k under different window size W is modeled as the transition gain $G_{i\to k}$ which can be computed via Algorithm 1.

As shown in the *for* loop of Algorithm 1, the transition gain $G_{i\to k}$ is acquired by adopting the exhaustive search method, i.e., to scan from every enumerate possible middle union m. Furthermore, the bitwise AND operation of the possible middle union and the state index k will consistently be equal to k since the bit values that denote correctly received packets in the transmitter correctness bitmap will always have the one value. For example, it can be observed that the bitwise AND operation on the middle union $m = [101]$ and the original state index $k = [001]$ is still equivalent to the original state index $k = [001]$.

As a result, the algorithm employs the function *bitwise_and*() and the state index i as a mask to filter out those unsuitable middle unions m recognized by the discriminant that the bitwise AND operation of i and m is not equal to i. Moreover, the number of newly correctly acknowledged packets is represented as the variable α. The variable β records the number of the remaining zeros, i.e., the number of those unacknowledged packets. The two variables α and β are utilized for the computation of packet error probability based on the corresponding middle union m. For the next step, the *while* loop generates the resulting state index r by the rule to suppress all leading one of the middle union m and to pad an equal number of zeros from the right-hand side. Consequently, the transition gain $G_{i\to k}$ can be computed via the sum of error probability from each suitable middle union m leading to the resulting state index $r = k$.

3.1.4 Window utilization

The window utilization for the GS scheme can be derived from the saturated probability of internal states after the occurrence of an infinite number of state transitions. The saturated probability Θ_k for each internal state S_k under the

Algorithm 1: *Computation of Transition Gain for Greedy Scheme*

```
Data: i, k, and r are unsigned binary integers of W digits
Result: G_{i→k}
begin
    G_{i→k} ⟵ 0;
    for m ⟵ 0 to 2^W − 1 do
        if i = bitwise_and(i, m) then
            α ⟵ number_of_one(m) − number_of_one(i);
            β ⟵ number_of_zero(m);
            r = m;
            while leftmost_bit(r) = 1 do
                shift r one bit left with zero padding;
            end
            if r = k then
                G_{i→k} ⟵ G_{i→k} + (1 − p_e)^α p_e^β;
            end
        end
    end
end
```

window size W can be computed as the sum of all the possible 2^{W-1} state transitions as

$$\Theta_k = \sum_{i=0}^{2^{W-1}-1} G_{i\to k}\Theta_i, \tag{1}$$

for $\forall k \in [0, 1, \ldots, 2^{W-1}-1]$. However, these state equations form an underdetermined linear system which has an infinite number of solutions for all the Θ_k. Therefore, for solving the saturated probability Θ_k, an additional constraint is imposed in order to make the underdetermined system possess a finite number of solutions, i.e.,

$$\sum_{k=0}^{2^{W-1}-1} \Theta_k = 1 \tag{2}$$

since the sum of all saturated state probability Θ_k in a Markov state transition diagram should be equal to one. After the derivation of saturated probability Θ_k from (1) and (2), the window utilization U_G^W of the GS scheme under the window size W can be obtained as

$$U_{GS}^W = \frac{\sum_{k=0}^{2^{W-1}-1}(1-p_e)Z_W(k)\Theta_k}{W}. \tag{3}$$

where the subscript GS is adopted to denote the conventional GS scheme. $Z_W(k)$ represents the number of zeros within the state index k of W digits, i.e., to indicate the number of unacknowledged data packets. It is noted that the product $(1-p_e)\cdot Z_W(k)$ denotes the expected total number of properly acknowledged data packets that is forecasted in the next state transition of S_k.

An illustrative example under the window size $W = 3$ is provided as follows. Based on (1), the four state equations under $W = 3$ are represented via the matrix form as

$$\begin{bmatrix}\Theta_0\\ \Theta_1\\ \Theta_2\\ \Theta_3\end{bmatrix} = \begin{bmatrix} 1-2p_e+2p_e^2 & (p_e-1)^2 & 1-p_e & 1-p_e\\ (1-p_e)p_e^2 & p_e^2 & 0 & 0\\ p_e(1-p_e) & p_e(1-p_e) & p_e^2 & 0\\ p_e(p_e-1)^2 & (1-p_e)p_e & (1-p_e)p_e & p_e \end{bmatrix}\begin{bmatrix}\Theta_0\\ \Theta_1\\ \Theta_2\\ \Theta_3\end{bmatrix}. \tag{4}$$

Associated with $\sum_{k=0}^{3}\Theta_k = 1$, the solution for each saturated probability Θ_k of S_k can be obtained as

$$\Theta_0 = \frac{1+p_e}{1+3p_e+2p_e^2+p_e^3} \tag{5}$$

$$\Theta_1 = \frac{p_e^2}{1+3p_e+2p_e^2+p_e^3} \tag{6}$$

$$\Theta_2 = \frac{p_e(1+p_e+p_e^2)}{1+4p_e+5p_e^2+3p_e^3+p_e^4} \tag{7}$$

$$\Theta_3 = \frac{p_e(1+2p_e+p_e^2+p_e^3)}{1+4p_e+5p_e^2+3p_e^3+p_e^4} \tag{8}$$

if $p_e \neq 1$. In the case of $p_e = 1$, it can be acquired that $\Theta_0 = 1$ and $\Theta_1 = \Theta_2 = \Theta_3 = 0$. As a result, the window utilization for the $W = 3$ case becomes

$$\begin{aligned} U_{GS}^3 &= \frac{(1-p_e)(3\Theta_0+2\Theta_1+2\Theta_2+\Theta_3)}{3}\\ &= \frac{3+6p_e-4p_e^3-4p_e^4-p_e^5}{3+12p_e+15p_e^2+9p_e^3+3p_e^4}, \end{aligned} \tag{9}$$

which concludes the description and derivation of the analytical model for conventional GS scheme.

3.2 Analytical model for proposed greedy fast-shift scheme

The derivation of the analytical model for proposed GFS scheme is similar to that of the conventional GS scheme in the aspect of adopting the Markov chain techniques. Accordingly, the internal states, the state transition diagram, and the corresponding state transition probability will first be described and properly defined. With the help of these defined elements, the analytical model for the GFS scheme is concluded by the mathematical expression of window utilization, and all the context will be provided by a generic analytical model for the window size W with an illustrative example under $W = 3$.

3.2.1 Internal states

In order to define the internal states of the proposed GFS scheme, five parameters should be introduced including (a) the transmitter correctness bitmap, (b) the receiver correctness bitmap, (c) the state index, (d) the correctness array, and (e) the middle union. The transmitter and receiver correctness bitmaps respectively represent the Boolean correctness array for all numbered data packets from the transmitter's and the receiver's perspectives. The state index is defined as a set of $2W-1$ binary digits with its most significant bit at the first zero of the receiver correctness bitmap. Noticed that the state index for the proposed GFS scheme is defined from the receiver's perspective instead of the transmitter's aspect as in the GS

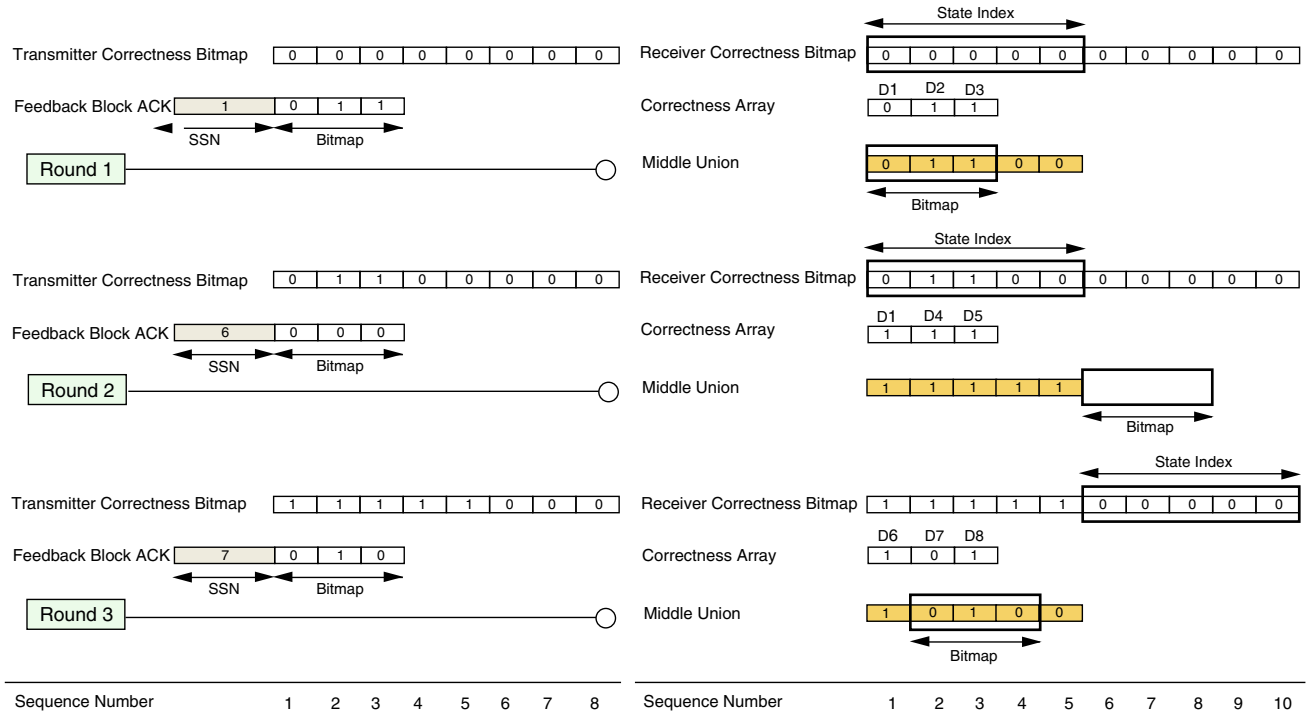

Fig. 4 The five critical parameters for the internal state definition of the proposed GFS scheme: the transmitter correctness bitmap, the receiver correctness bitmap, the correctness array, the middle union, and the state index

scheme. The correctness array represents the situations whether the individual data packet in the current aggregate frame is successfully received or not. In the end, the middle union is defined as the combined result of the current state index and the correctness array. The combination is conducted by setting the corresponding bit in the current state index if the data packet is specified as correctly received by the correctness array. It is noted that the middle union also has the size of $2W - 1$ digits.

The illustrative example under the window size $W = 3$ is shown in Fig. 4. Initially, in the first round, both the transmitter and the receiver correctness bitmaps are all-zero arrays, which result in the state index $k = [00000]$. Noted that the size of state index becomes $2W - 1 = 5$. The transmitter starts to deliver the numbered data packets from D1 to D3. Assuming the correctness array as $c = [011]$ which denotes that only the first packet D1 is corrupted, the middle union will become $m = [01100]$ since the corresponding fields for D2 and D3 in the state index are set to be 1. In the same time, based on the definition that the most significant bit of the state index must be the first zero of the receiver correctness bitmap, the new state index will therefore be $k = [01100]$ as shown in the second round of Fig. 4. According to the proposed GFS algorithm, the receiver will choose SSN to be the SN of the first unacknowledged packet, i.e., the packet D1. Consequently, the receiver will send the block ACK with SSN $= 1$ and the bitmap $b = [011]$ back to the transmitter.

After the reception of feedback block ACK packet, the transmitter correctness bitmap is updated as shown in the second round of Fig. 4. Therefore, the transmitter will send the previously corrupted packet D1 associated with new-coming packets D4 and D5 to the receiver. If the correctness array is $c = [111]$, i.e., all packets are correct, the middle union will become $m = [11111]$ since packets D1, D4 and D5 are correctly received. The new state index will therefore be right shifted five digits and become $k = [00000]$ as in the third round. Based on the GFS scheme, the SSN of the feedback block ACK packet in the second round will become 6 and the corresponding bitmap will be $b = [000]$. From the transmitter side, SSN $= 6$ indicates that all packets before D6 are successfully received. Therefore, the first five digits of the transmitter correctness bitmap are all 1 as in the third round of Fig. 4. The procedures will be repeatedly conducted if there is any data packet to be transmitted.

The reason for the state index to contain $2W - 1$ digits is stated as follows. Consider the worst case that the transmitter delivers an aggregate frame with W packets and only the first packet is failed to be transmitted. The transmitter will retransmit the failed first packet together with the other $W - 1$ new-coming packets. Therefore, from the receiver's perspective, the number of influenced digits in the receiver correctness bitmap will be $2W - 1$, which also represents the total number of involved $W + (W - 1)$ data packets during the transmissions.

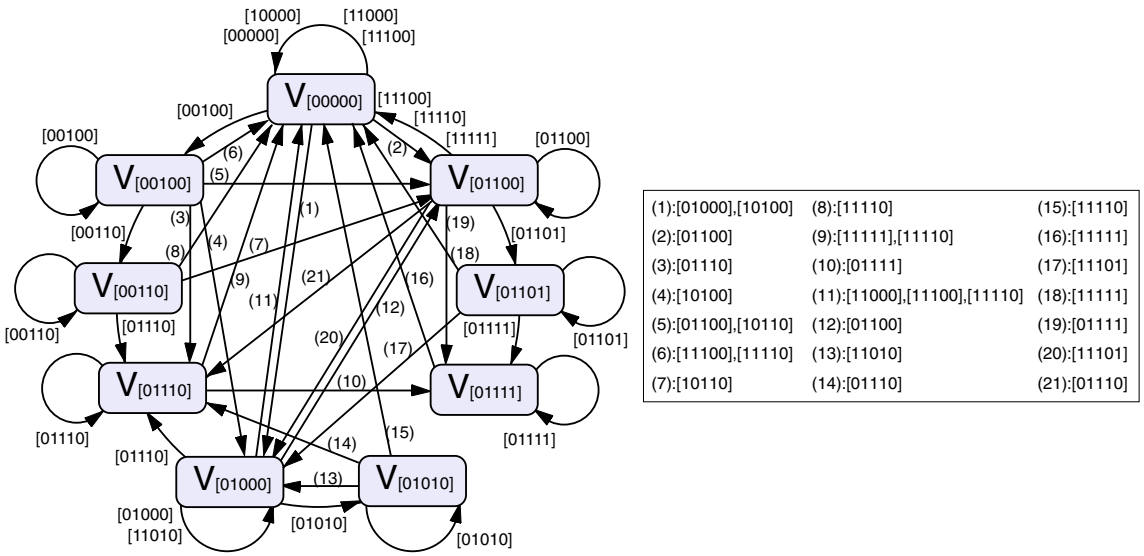

Fig. 5 State transition diagram for the proposed GFS scheme under the window size $W = 3$: Each state transition is represented as a unidirectional link with the causal middle union of width $2W - 1$

Moreover, it is required to figure out the total number of state indexes and that for the corresponding internal states. The leftmost bit of the state index is always zero according to the definition of state index. The remaining $W - 1$ digits of the state index control the number of new-coming packets in the next aggregate frame. Therefore, these $W - 1$ digits are responsible for the calculation of total number of internal states. In the case that none of these $W - 1$ digits is zero, the transmitter will transmit $W - 1$ new-coming packets which results in the total number of state indexes as $C_0^{W-1}2^{W-1}$, where C_a^b is denoted as the binomial coefficient. If one of these $W - 1$ digits is zero, the transmitter will retransmit the failed packets with $W - 2$ new-coming packets which will cause an additional number of $C_1^{W-1}2^{W-2}$ state indexes. As a result, the total number of state indexes or internal states can be generalized and obtained as

$$N_{GFS}^{W} = \sum_{i=0}^{W-1} C_i^{W-1} 2^{W-1-i}. \tag{10}$$

The proposed GFS scheme has N_{GFS}^{W} internal states that are denoted as V_k with the index $k \in \mathbb{I}$, where $\mathbb{I}$ is the set of all state indexes. As shown in Fig. 5, the nine internal states $V_{[00000]}, V_{[00100]}, V_{[01100]}, V_{[01000]}, V_{[00110]}, V_{[01110]}, V_{[01101]}$, $V_{[01111]}$, and $V_{[01010]}$ are depicted in the state transition diagram for the proposed GFS scheme under the window size $W = 3$.

3.2.2 State transition diagram

The state transition diagram of GFS scheme under the window size W consists of N_{GFS}^{W} internal states and their possible state transitions. The exemplified state transition diagram under window size $W = 3$ is illustrated in Fig. 5. Each transition between two states is represented as a unidirectional link from the original state V_i to the resulting state V_k. Moreover, the middle unions that result in the state transitions are also shown around the link. For example, the state transition from $V_{[00100]}$ to $V_{[01000]}$ is obtained according to the middle union $m = [10100]$. This middle union $m = [10100]$ will consequently let the receiver increase the SSN by one, causing the state index to become $k = [01000]$, i.e., the state of $V_{[01000]}$. The state $V_{[01000]}$ can be obtained by suppressing all the leading ones within the middle union and padding an equal number of zeros from the right-hand side, which is considered the same technique as in the conventional GS scheme.

3.2.3 State transition probability

As shown in Fig. 5, the transition probability from the initial state $V_{[00100]}$ to the resulting state $V_{[01000]}$ can be computed from the bit values within the corresponding middle union $m = [10100]$. According to the initial state $V_{[00100]}$ and the window size $W = 3$, the transmitter will send an aggregate frame consisting of two previously corrupted packets and one new-coming packet. These packets are respectively represented by the first two bits and the fourth bit from the left-hand side since the third bit denotes the correctly received packet in the last aggregate frame. Accordingly, referring to the middle union $m = [10100]$, the casual correctness array can be obtained by its first two bits and the fourth bit as $c = [100]$. The transition gain from $V_{[00100]}$ to $V_{[01000]}$ is therefore computed by the probability of the correctness array $c = [100]$

and is denoted as $H_{[00100]\to[01000]} = (1-p_e)\cdot p_e^2$, where p_e is the packet error probability. The generic transition probability from V_i to V_k under different window size W is modeled as the transition gain $H_{i\to k}$ which can be computed via Algorithm 2.

Algorithm 2: *Computation of Transition Gain for Greedy Fast-Shift Scheme*

```
Data: i, k, and r are unsigned binary integers of 2W − 1 digits
Result: H_{i→k}
begin
    H_{i→k} ⟵ 0;
    γ ⟵ number_of_zero_in_the_leftmost_W_bits(i) − 1;
    for s ⟵ 0 to 2^{2W−1−γ} − 1 do
        m ⟵ s_with_γ_zero_paddings_from_right_hand_side;
        if i = bitwise_and(i, m) then
            α ⟵ number_of_one(m) − number_of_one(i);
            β ⟵ number_of_zero(m) − γ;
            r = m;
            while leftmost_bit(r) = 1 do
                shift r one bit left with zero padding;
            end
            if r = k then
                H_{i→k} ⟵ H_{i→k} + (1 − p_e)^α p_e^β;
            end
        end
    end
end
```

The main idea of Algorithm 2 is to find the probability sum of all possible middle unions which can let the state V_i change to the state V_k. the algorithm first sets a parameter γ to record the number of zeros within W digits from the left-hand side of state index i, excluding the leftmost leading zero. The physical meaning of γ is to specify the number of zeros from the right-hand side of the state index since these zeros represent those packets that have not been transmitted. The remaining $2W-1-\gamma$ digits from the left-hand side of state index i is the only portion that can influence the state transition. Therefore, as shown in Algorithm 2, the variable s of the *for* loop represents all possible bit patterns within $2W-1-\gamma$ digits. All the possible middle union m can be obtained with γ zero paddings from the right-hand side. The bitwise AND operation of these middle unions with the state index i can filter out the unsuitable middle unions m recognized by the discriminant that the bitwise AND operation of i and m is not equal to i. With regard to the state index i and the middle union m, the variable α represents the newly correctly received packets; while β indicates the number of unacknowledged packets. The value of β can be obtained by subtracting the total number of remaining zeros with the γ zeros from right-hand side. The probability for the middle union can therefore be formulated as $(1-p_e)^{\alpha}\cdot p_e^{\beta}$. Subsequently, the *while* loop generates the resulting state index by the rule of suppressing the leading one and padding an equal number of zeros. Finally, the transition gain $H_{i\to k}$ can be computed via the sum of probability from each suitable middle union m leading to the resulting state index $r = k$.

3.2.4 Window utilization

The window utilization for proposed GFS scheme can be derived from the saturated probability of internal states after the occurrence of an infinite number of state transitions. The saturated probability Λ_k for each internal state V_k under the window size W can be computed as the sum of all the possible state transition as

$$\Lambda_k = \textstyle\sum_{i\in\mathbb{I}} H_{i\to k}\Lambda_i \tag{11}$$

for $\forall k \in \mathbb{I}$, where $\mathbb{I}$ is the set of all state indexes. Similarly, in order to solve the saturated probability Λ_k, an additional constraint is imposed to make the underdetermined system possess a finite number of solutions, i.e.,

$$\sum_{k\in\mathbb{I}} \Lambda_k = 1, \tag{12}$$

since the sum of all saturated state probability Λ_k in a Markov state transition diagram should be equal to one. Based on (11), the nine state equations derived from the exemplified state transition diagram under $W = 3$ are represented via the matrix form as

$$\mathbf{\Lambda} = [\mathbf{A}|\mathbf{B}]_{9\times 9}\,\mathbf{\Lambda}, \tag{13}$$

where $\mathbf{\Lambda} = \left[\Lambda_{[00000]}\ \Lambda_{[00100]}\ \Lambda_{[01100]}\ \Lambda_{[01000]}\ \Lambda_{[00110]}\ \Lambda_{[01110]}\ \Lambda_{[01101]}\ \Lambda_{[01111]}\ \Lambda_{[01010]}\right]^T$ with

$$\mathbf{A}_{9\times4}=\begin{bmatrix} 2p_e^2-2p_e+1 & 1-2p_e+p_e^2 & 1-2p_e+2p_e^2-p_e^3 & 1-2p_e+2p_e^2-p_e^3 \\ p_e^2-p_e^3 & p_e^3 & 0 & 0 \\ p_e-2p_e^2+p_e^3 & p_e-p_e^2 & p_e^3 & p_e^2-p_e^3 \\ p_e-p_e^2 & p_e^2-p_e^3 & p_e-2p_e^2+p_e^3 & p_e-2p_e^2+2p_e^3 \\ 0 & p_e^2-p_e^3 & 0 & 0 \\ 0 & p_e-2p_e^2+p_e^3 & p_e^2-p_e^3 & p_e-2p_e^2+p_e^3 \\ 0 & 0 & p_e^2-p_e^3 & 0 \\ 0 & 0 & p_e-2p_e^2+p_e^3 & 0 \\ 0 & 0 & 0 & p_e^2-p_e^3 \end{bmatrix} \tag{14}$$

and

$$\mathbf{B}_{9\times5}=\begin{bmatrix} 1-2p_e+p_e^2 & 1-p_e & 1-2p_e+p_e^2 & 1-p_e & 1-2p_e+p_e^2 \\ 0 & 0 & 0 & 0 & 0 \\ p_e-p_e^2 & 0 & 0 & 0 & 0 \\ 0 & 0 & p_e-p_e^2 & 0 & p_e-p_e^2 \\ p_e^2 & 0 & 0 & 0 & 0 \\ p_e-p_e^2 & p_e^2 & 0 & 0 & p_e-p_e^2 \\ 0 & 0 & p_e^2 & 0 & 0 \\ 0 & p_e-p_e^2 & p_e-p_e^2 & p_e & 0 \\ 0 & 0 & 0 & 0 & p_e^2 \end{bmatrix}. \tag{15}$$

Associated with (12), if $p_e \neq 1$, the solution for each saturated probability Λ_k of V_k can be obtained as

$$\begin{bmatrix} \Lambda_{[00000]} \\ \Lambda_{[00100]} \\ \Lambda_{[01100]} \\ \Lambda_{[01000]} \\ \Lambda_{[00110]} \\ \Lambda_{[01110]} \\ \Lambda_{[01101]} \\ \Lambda_{[01111]} \\ \Lambda_{[01010]} \end{bmatrix} = \begin{bmatrix} \frac{(p_e^3+2p_e^2+2p_e+1)(p_e^5+3p_e^4+3p_e^3+4p_e^2+2p_e^+1)}{C_1(p_e)} \\ \frac{p_e^2(p_e+1)(p_e^5+3p_e^4+3p_e^3+4p_e^2+2p_e+1)}{C_1(p_e)} \\ \frac{p_e(p_e^7+3p_e^6+5p_e^5+7p_e^4+7p_e^3+5p_e^2+2p_e+1)}{C_1(p_e)} \\ \frac{p_e(p_e^7+4p_e^6+8p_e^5+11p_e^4+12p_e^3+9p_e^2+5p_e+1)}{C_1(p_e)} \\ \frac{p_e^4(p_e^5+3p_e^4+4p_e^2+2p_r+1)}{C_1(p_e)} \\ \frac{p_e^2(p_e^2+p_e+1)(p_e^7+3p_e^6+6p_e^5+11p_e^4+11p_e^3+8p_e^2+6p_e+1)}{(p_e+1)C_2(p_e)} \\ \frac{p_e^3(p_e^7+3p_e^6+5p_e^5+7p_e^4+7p_e^3+5p_e^2+2p_e+1)}{(p_e+1)C_1(p_e)} \\ \frac{p_e^2(p_e^2+p_e+1)(p_e^7+3p_e^6+6p_e^5+11p_e^4+11p_e^3+8p_e^2+6p_e+1)}{(p_e+1)C_2(p_e)} \\ \frac{p_e^3(p_e^7+4p_e^6+8p_e^5+11p_e^4+12p_e^3+9p_e^2+5p_e+1)}{C_2(p_e)} \end{bmatrix}, \tag{16}$$

where

$$C_1(p_e) = p_e^{10} + 6p_e^9 + 20p_e^8 + 42p_e^7 + 62p_e^6 + 72p_e^5 + 63p_e^4 + 42p_e^3 + 20p_e^2 + 6p_e + 1$$
$$C_2(p_e) = p_e^{11} + 7p_e^{10} + 26p_e^9 + 62p_e^8 + 104p_e^7 + 134p_e^6 + 135p_e^5 + 105p_e^4 + 62p_e^3 + 26p_e^2 + 7p_e + 1. \quad (17)$$

$$U_{GFS}^3 = \frac{C_3(p_e) + 105p_e^7 - 41p_e^6 - 168p_e^5 - 201p_e^4 - 151p_e^3 - 72p_e^2 - 21p_e - 3}{-3(p_e+1)C_2(p_e)}, \quad (20)$$

In the case that $p_e = 1$, it is acquired that $\Lambda_{[00000]} = 1$ and the others are equal to 0.

After the derivation of saturated probability Λ_k from (11) and (12), the window utilization U_{GFS}^W of the proposed GFS scheme under the window size W can be obtained as

$$U_{GFS}^W = \sum_{k\in\mathbb{I}} \frac{E[N_{new}^k]\Lambda_k}{W}, \quad (18)$$

where $E[N_{new}^k]$ represents the expected total number of newly acknowledged data packets that is forecasted in the next state transition of S_k. It can be computed as

$$E[N_{new}^k] = \sum_{j\in\mathbb{M}_k} P_W^j(k) S_W^j(k), \quad (19)$$

where $\mathbb{M}_k$ is the set of all possible middle union outgoing from the state V_k. The parameter $P_W^j(k)$ denotes the probability of the corresponding outgoing middle union j; while $S_W^j(k)$ denotes the newly acknowledged data packets under the same middle union j. As shown in Fig. 5, for example, the middle union $j = [01110]$ is one of the outgoing middle unions from the state $V_{[00110]}$. Based on the state index, two corrupted packets and one new-coming packet will be delivered since the transmitter can only recognize the first $W = 3$ bits due to the window size constraint. Moreover, the fourth bit as 1 represents the data packet that is previously correctly received but not properly acknowledged. The last bit will remain 0 since the next aggregate frame transmission will not include the corresponding packet. Finally, according to the middle union $j = [01110]$, the correctness array becomes $c = [01X]$ where X is denoted as the don't-care bit. Therefore, $P_W^j(k)$ can be obtained as $p_e \cdot (1 - p_e)$; while $S_W^j(k)$ is computed as 1 since only one packet is newly acknowledged as correct. Consider another middle union $j = [11110]$ of the same state $V_{[00110]}$, the correctness array will be $c = [11X]$ associated with $P_W^j(k) = (1 - p_e)^2$ and $S_W^j(k) = 3$. The reason for $S_W^j(k) = 3$ is that the previously correctly received data packet denoted by the fourth bit in the state index can be detected as correct in conjunction with the two correct packet receptions in the current aggregate frame. According to (18) and (19), the window utilization for the exemplified state transition diagram of $W = 3$ can be obtained as

where $C_2(p_e)$ is specified in (17) and

$$C_3(p_e) = p_e^{13} + 11p_e^{12} + 47p_e^{11} + 117p_e^{10} + 186p_e^9 + 190p_e^8. \quad (21)$$

It concludes the description and derivation of the analytical model for proposed GFS scheme.

4 Performance evaluation

In this section, model validation of the proposed analytical models for both the conventional GS mechanism and the proposed GFS scheme is conducted via the simulations. Furthermore, the comparison between these two schemes is performed under different simulation scenarios. The network scenario includes one base station (BS) and multiple channel contenders, where the channel contenders are randomly placed within the transmission range of the BS. The simulations are conducted in the network simulator (NS-2, [32]) with wireless extension, using the IEEE 802.11n distributed coordination function (DCF) as the MAC protocol. The parameters utilized in the simulations are listed as shown in Table 1.

4.1 Model validation

In order to illustrate the effectiveness of proposed analytical models, both block ACK mechanisms are validated with simulation results. The window utilization which is defined as the average number of successfully acknowledged packets of an aggregate frame divided by the window size W is utilized as the validation index. Figures 6 and 7 illustrate the comparison for window utilization W with different packet error probabilities p_e under the window size $W = 3$ and 6, respectively. It can be observed that

the proposed theoretical models can almost match and predict the performance of the two schemes via simulation results, which validates the correctness of proposed models. Furthermore, in the performance comparison between the two schemes based on the metric of window utilization, Figs. 6 and 7 show that the proposed GFS scheme outperforms the conventional GS mechanism under both window size $W = 3$ and $W = 6$.

The performance gaps between the proposed GFS scheme and the GS method can be attributed to the different ACK feedback mechanisms. In additional to providing explicit ACK to each packet in the aggregate frame after the SSN, the proposed GFS scheme furthermore implicitly acknowledges the correctly received packets before the SSN. Contributing to this hybrid method, the SSN in the proposed GFS scheme will slide faster than that in the GS mechanism which results in higher window utilization. All the performance curves in Figs. 6 and 7 have the trend that the window utilization is degraded with the increase of packet error probability p_e. Intuitively, as p_e becomes larger, more packet errors will occur which consequently decrease the window utilization.

Table 1 Simulation parameters

Parameter type	Parameter value
Network area	Disk with a radius of 250 m
Simulation time	40 s
Transmission range	250 m
Routing protocol	DumbAgent
Traffic type	Constant bit rate (CBR)
Data packet size	500 bytes
Number of base station	1
Number of channel contender	5, 10, 15
Queue size	100 packets
PHY data rate	100 Mbps

4.2 Performance comparison

For the purpose of comparing the performance between the GFS and the GS mechanisms, three performance metrics are utilized in the simulations as follows.

1. Blocking Overhead: The number of additional data packets per second which have been retransmitted due to the insufficient window size.
2. End-to-End Delay: the duration between the time when the packet arrives at the transmitter queue and the time when the packet is successfully acknowledged by the receiver.
3. Throughput: the total number of successfully received packets per second.

The comparisons between the proposed GFS scheme and the conventional GS mechanism under these three metrics will be performed under different window sizes W, packet error probabilities p_e, and numbers of contending nodes N.

Figures 8, 9 and 10 show the performance comparison based on the three metrics versus packet error probability with window size $W = 64$ under the number of contending nodes $N = 5, 10$, and 15. Figure 8 illustrates the comparison of blocking overhead between the proposed GFS scheme and the GS method. The blocking overhead becomes smaller with the increased number of nodes, which can be contributed to the smaller system throughput caused by higher packet collisions from more contending nodes. With lowered throughput performance, the chance for the occurrence of additional retransmitted packets will

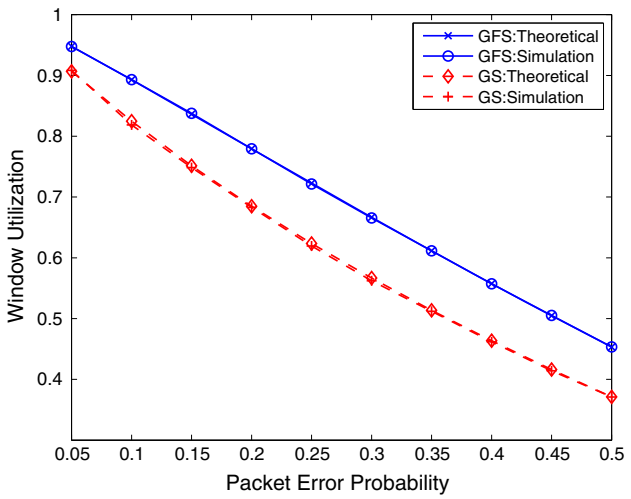

Fig. 6 Model validation: window utilization versus packet error probability under window size $W = 3$

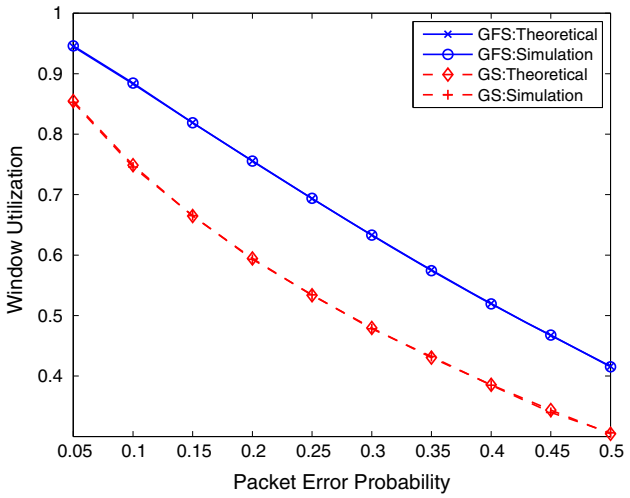

Fig. 7 Model validation: window utilization versus packet error probability under window size $W = 6$

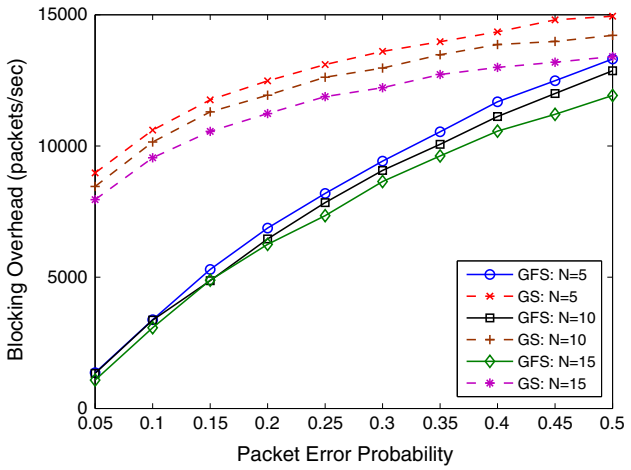

Fig. 8 Performance comparison: blocking overhead versus packet error probability under the window size $W = 64$

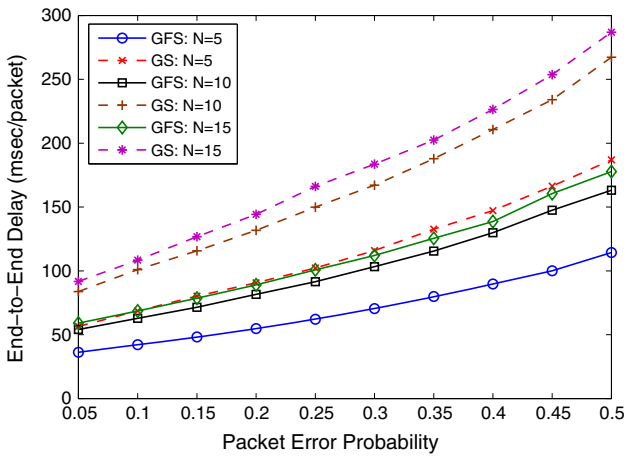

Fig. 9 Performance comparison: end-to-end delay versus packet error probability under the window size $W = 64$

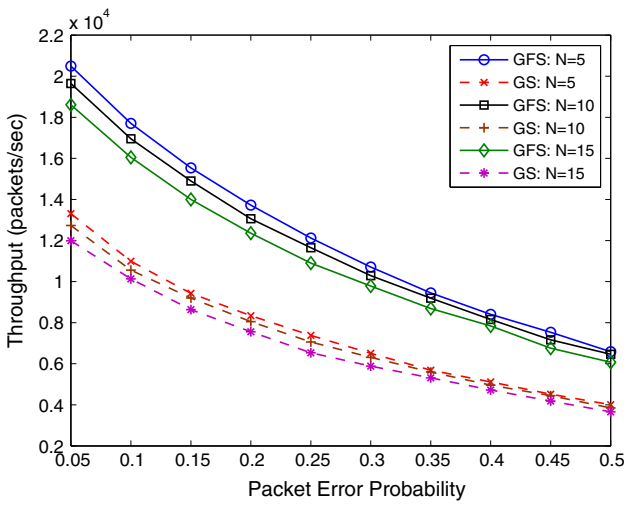

Fig. 10 Performance comparison: throughput versus packet error probability under the window size $W = 64$

consequently be reduced. It is also observed that the blocking overhead becomes larger with regard to the increase of packet error probability. As the packet error happens frequently, it becomes difficult to enlarge the SSN value in the block ACK packet which causes more packets outside of the ACK window, i.e., from SSN to $\text{SSN} + (W - 1)$, to be retransmitted. Furthermore, as shown in Fig. 8, the proposed GFS scheme outperforms the GS method due to its fast-shift mechanism for packet acknowledgements, which consequently reduce the number of retransmitted blocked packets. In the proposed GFS scheme, the receiver can shift the SSN to the maximal value of $2W - 1$; while the GS method can only increase the SSN value up to W. As a result, the proposed GFS scheme will cause less blocking overhead compared to the GS method.

The end-to-end delay under different packet error probabilities and numbers of nodes is shown in Fig. 9. It is intuitively to notice that as the number of contending nodes is increased, more packet collisions and retransmissions will consequently occur leading to the enlargement of packet delay. Based on the same reason, the delay will be prolonged with regard to the increase of packet error probability since more retransmissions will be required. As shown in Figs. 6, 7 and 8, the proposed GFS scheme has higher window utilization and smaller blocking overhead compared to that from the conventional GS method. Therefore, more packets can be successfully transmitted in one aggregate frame by adopting the GFS scheme, which results in the shorter delay as shown in Fig. 9.

Figure 10 illustrates the comparison of throughput performance between the proposed GFS scheme and the GS method. It is observed that the system throughput is decreased as the packet error probability is augmented since more transmission attempts will be required to recover the packet errors. Moreover, the throughput performance is decreased in both schemes with the increased number of nodes, which is contributed to the additional packet collisions if there exists more channel contenders. Based on (3) and (18) and Figs. 6 and 7, the window utilization of the proposed GFS scheme is larger than the conventional GS scheme. Therefore, as shown in Fig. 10, the system throughput of the proposed GFS scheme will be higher than that of the GS method since the window utilization is a positive-related metric with respect to the throughput performance. This result further validates the effectiveness of our proposed analytical models and the analysis based on window utilization.

Figures 11, 12 and 13 depict the comparison with respect to the three metrics versus window size with packet error probability $p_e = 0.1$ under the number of contending nodes $N = 5, 10$, and 15. Figure 11 shows the blocking overhead performance for the proposed GFS and the

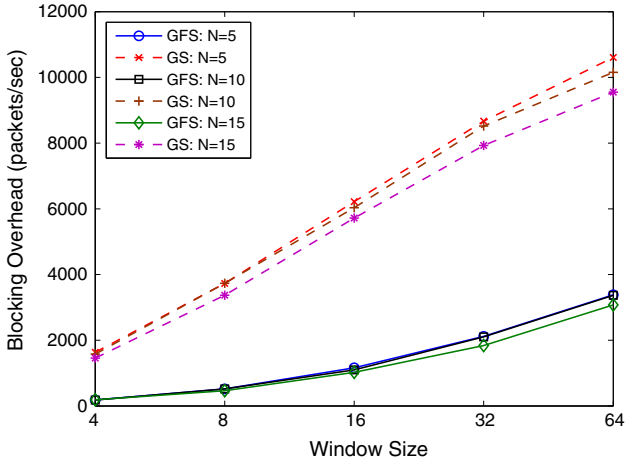

Fig. 11 Performance comparison: blocking overhead versus window size under packet error probability $p_e = 0.1$

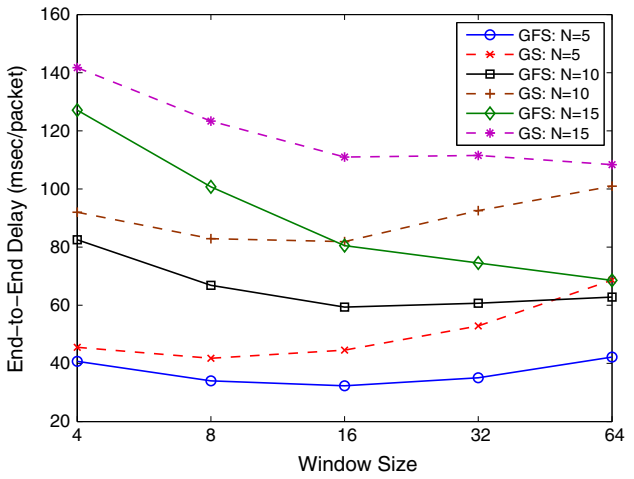

Fig. 12 Performance comparison: end-to-end delay versus window size under packet error probability $p_e = 0.1$

conventional GS schemes. It is observed that the blocking overhead becomes larger when the window size is extended, which can be explained as follows. From the transmitter side, consider that the SSN ξ_o of the block ACK packet is known, the packet with SN in the range from ξ_o to $\xi_o + (2W - 1)$ will possibly be included in the aggregate frame for the next transmission. After the receiver receives the aggregate frame, a new SSN ξ_n will be created. There is potential for the packets with SN in the range from $\xi_n + W$ to $\xi_o + (2W - 1)$ to induce the blocking overhead. As the window size increases, this range will be extended which consequently results in more blocking overhead. Nevertheless, the proposed GFS scheme causes significant less blocking overhead compared to the GS method owing to its efficient determination of the SSN value, which has been described as the explanation for Fig. 8.

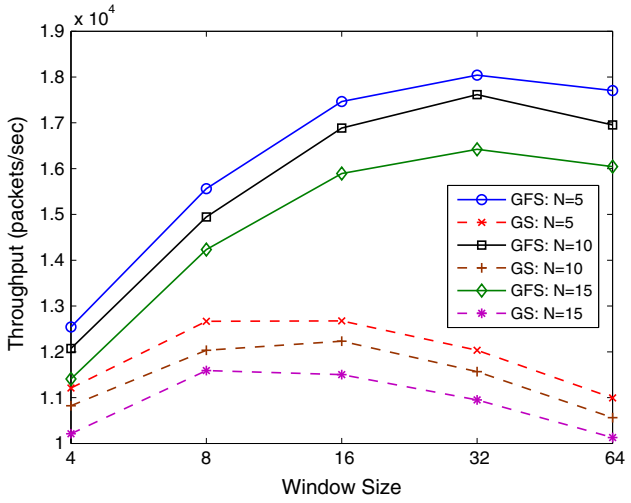

Fig. 13 Performance comparison: throughput versus window size under packet error probability $p_e = 0.1$

The end-to-end delay performance under different window sizes and number of nodes is shown in Fig. 12. As the window size becomes larger, there are two situations to happen which are explained as follows: (a) Since each aggregate frame can accommodate more packets, the end-to-end delay is decreased for the reason that packets will spend less time in the transmitter's queue; (b) With increased blocking overhead as in Fig. 11, additional time is required for the packets to be successfully acknowledged which contributes to larger packet delay. Based on the joint effects from these two cases, the end-to-end delay will be observed to first decrease and then increase as the window size is enlarged. Moreover, owing to the smaller blocking overhead and larger window utilization, the proposed GFS scheme possesses smaller end-to-end delay compared to the GS method. From the delay performance of Fig. 12, the evaluation on the throughput metric of Fig. 13 can be predicted and explained in a similar manner. As the window size becomes larger, the throughput performance of both schemes will first be increased and then decreased afterwards. Similar to the reason as explained in Fig. 10, due to the less blocking overhead and higher window utilization, the proposed GFS scheme will have significant throughput gain in comparison with the conventional GS method. The effectiveness of the proposed mechanism and analytical models can therefore be perceived, which concludes the performance evaluation of this section.

5 Conclusion

In this paper, a GFS block ACK mechanism is proposed to alleviate the performance degradation due to insufficient bitmap within the ACK window. Instead of adopting the

transmitter-defined SSN in the conventional greedy block ACK scheme, the design of receiver-defined SSN is utilized in the proposed GFS scheme. The proposed mechanism can effectively reduce the occurrence of packet retransmissions for those correctly received packets that are outside of the ACK window. Moreover, based on the Markovian techniques, the analytical models for both schemes are also constructed to measure the throughput-related performance metric, i.e., the window utilization. Simulations are performed to validate the proposed analytical models and to evaluate the performance for these two schemes. It can be observed from the performance comparison that the proposed GFS scheme can outperform the conventional greedy scheme on the throughput, delay, and blocking overhead under different window sizes and packet error probabilities.

Acknowledgments This work was in part funded by the Aiming for the Top University and Elite Research Center Development Plan, the Technological University Paradigms, NSC 102-2221-E-027-004, NSC 102-2221-E-009-018-MY3, the MediaTek research center at National Chiao Tung University, and the Telecommunication Laboratories at Chunghwa Telecom Co. Ltd, Taiwan.

References

1. IEEE 802.11 WG. (2003). IEEE Std 802.11a-1999(R2003): Part 11: Wireless LAN medium access control (MAC) and physical layer (PHY) specifications: High-speed physical layer in the 5 GHz Band, IEEE Standards Association Std.
2. IEEE 802.11 WG (2003). IEEE Std 802.11b-1999(R2003): Part 11: Wireless LAN medium access control (MAC) and physical layer (PHY) specifications: Higher-speed physical layer extension in the 2.4 GHz Band, IEEE Standards Association Std.
3. IEEE 802.11 WG (2003). IEEE Std 802.11g-2003: Part 11: Wireless LAN medium access control (MAC) and physical layer (PHY) specifications: Amendment 4: Further higher data rate extension in the 2.4 GHz Band, IEEE Standards Association Std.
4. IEEE 802.11 WG (2005). IEEE Std 802.11e-2005: Part 11: Wireless LAN Medium Access Control (MAC) and Physical Layer (PHY) Specifications: Amendment 8: Medium Access Control (MAC) Quality of Service Enhancements, IEEE Standards Association Std.
5. IEEE 802.11 WG (2009). IEEE 802.11n-2009: Part 11: Wireless LAN medium access control (MAC) and physical layer (PHY) specifications: Amendment 5: Enhancements for higher throughput, IEEE Standards Association Std.
6. Heiskala, J., & Terry, J. (2001). *OFDM wireless LANs: A theoretical and practical guide*.Indianapolis, IN: Sams.
7. Tse, D., & Viswanath, P. (2005). *Fundamentals of wireless communication*. Cambridge: Cambridge University Press.
8. Xiao, Y., & Rosdahl, J. (2002). Throughput and delay limits of IEEE 802.11. *IEEE Communications Letters*, *6*(8), 355–357.
9. Yang, X. (2004). Packing mechanisms for the IEEE 802.11n wireless LANs. In *Proceedings of IEEE global telecommunications conference (GLOBECOM)* (pp. 3275–3279).
10. Lu, Y., Zhang, C., Lu, J., & Lin, X. (2007). A MAC queue aggregation scheme for VoIP transmission in WLAN. In *Proceedings of IEEE wireless communications and networking conference (WCNC)* (pp. 2121–2125).
11. Wu, Y. (2006). Multilevel modulation based differentiated data aggregation for wireless LANs. In *Proceedings of IEEE Region 10 Conference (TENCON)* (pp. 1–4).
12. Ghazisaidi, N., & Maier, M. (2010). Advanced aggregation techniques for integrated next-generation WLAN and EPON networks. In: *Proceedings of IEEE consumer communications and networking conference (CCNC)* (pp. 1–5).
13. Nguyen, S. H., Qazi, I. A., Andrew, L. L., & Vu, H. L. (2013). Rate equilibria in WLANs with block ACKs. In *Proceedings of IEEE LCN*.
14. Hajlaoui, N., Jabri, I., & Jemaa, M. B. (2013). Analytical study of frame aggregation in error-prone channels. In *IEEE wireless communications and mobile computing conference (IWCMC)* (pp. 237–242).
15. Chou, K.-H., & Lin, W. (2013). Performance analysis of packet aggregation for IEEE 802.11 PCF MAC-based wireless networks. *IEEE Transactions on Wireless Communication*, *12*(4), 1441–1447.
16. Abichar, Z., & Chang, J. (2013). Group-based medium access control for IEEE 802.11n Wireless LANs. *IEEE Transactions on Mobile Computing*, *12*(2), 304–317.
17. Lin, J.-S., Feng, K.-T., Huang, Y.-Z., & Wang, L.-C. (2013). Novel design and analysis of aggregated ARQ protocols for IEEE 802.11n networks. *IEEE Transactions on Mobile Computing*, *12*(3), 556–570.
18. Feng, K.-T., Huang, Y.-Z., & Lin, J.-S. (2011). Design of MAC-defined aggregated ARQ schemes for IEEE 802.11n networks. *Wireless Networks*, *17*(3), 685–699.
19. Kramer, G. (2005). *Ethernet passive optical networks*. New York: Mcgraw-Hill.
20. Ghazisaidi, N., Maier, M., & Assi, C. M. (2009). Fiber-wireless (FiWi) sccess networks: A survey. *IEEE Communications Magazine*, *47*(2), 160–167.
21. Ginzburg, B., & Kesselman, A. (2007). Performance analysis of A-MPDU and A-MSDU aggregation in IEEE 802.11n. In *Proceedings of IEEE Sarnoff Symposium* (pp. 1–5).
22. Skordoulis, D., Ni, Q., Chen, H. H., Stephens, A. P., Liu, C., & Jamalipour, A. (2008). IEEE 802.11n MAC frame aggregation mechanisms for next-generation High-throughput WLANs. *IEEE Wireless Communications Magazine*, *15*(1), 40–47.
23. Kuo, Y. W. (2007). Throughput analysis for wireless LAN with frame aggregation under mixed traffic. In *Proceedings of IEEE region 10 conference* (TENCON) (pp. 1–4).
24. Kim, B. S., Hwang, H. Y., & Sung, D .K. (2008). Effect of frame aggregation on the throughput performance of IEEE 802.11n. In *Proceedings of IEEE wireless communications and networking conference (WCNC)* (pp. 1740–1744).
25. Lin, Y., & Wong, V. W. S. (2006). Frame aggregation and optimal frame size adaptation for IEEE 802.11n WLANs. In *Proc. IEEE global telecommunications conference (GLOBECOM)* (pp. 1–6).
26. Nagai, Y., Fujimura, A., Shirokura, Y., Isota, Y., Ishizu, F., Nakase, H., et al. (2006). 324Mbps WLAN equipment with MAC frame aggregation, In *Proceedings IEEE international symposium on personal, indoor and mobile radio communications (PIMRC)* (pp. 1–5).
27. Kim, Y., Choi, S., Jang, K., & Hwang, H. (2004). Throughput enhancement of IEEE 802.11 WLAN via frame aggregation. In *Proceedings of IEEE vehicular technology conference (VTC)*. (pp. 3030–3034).
28. Forouzan, B. A. (2006). *Data communications and networking*. New York: McGraw-Hill.
29. Nakajima, T., Nabetani, T., Utsunomiya, Y., Adachi, T., & Takagi, M. (2007). A simple and efficient selective repeat scheme for high throughput WLAN, IEEE802.11n. In *Proceedings of IEEE vehicular technology conference (VTC)* (pp. 1302–1306).

30. Nakajima, T., Utsunomiya, Y., Nishibayashi, Y., Tandai, T., Adachi, T., & Takagi, M. (2005). Compressed block ACK, an efficient selective repeat mechanism for IEEE802.11n. In *Proceedings of IEEE international symposium on personal, indoor and mobile radio communications (PIMRC)* (pp. 1479–1483).
31. Papoulis, A., & Pillai, S. U. (2002). *Probability, random variables, and stochastic processes* (4th ed.). New York: McGraw-Hill.
32. Heidemann, J., Bulusu, N., Elson, J., Intanagonwiwak, C., Lan, K., Xu, Y., Ye, W., Estrin, D., & Govindan, R. (2001). Effects of detail in wireless network simulation. In *Proceedings of SCS multiconference on distributed simulation* (pp. 3–11).

Wen-Jiunn Liu received his B.S. and Ph.D. degrees in communications engineering from National Chiao Tung University, Hsinchu, Taiwan, R.O.C., in Jun. 2005 and Jun. 2010, respectively. His current research interests include the mac and network protocol design for wireless sensor networks and broadband wireless networks. Since Oct. 2010, he has been with the Realtek Semiconductor Corp., Hsinchu, Taiwan, R.O.C., working on Wi-Fi protocol stack feature development. Since Dec. 2013, he has been with the MediaTek Inc., Hsinchu, Taiwan, R.O.C., targeting on 4G LTE protocol suites.

Chao-Hua Huang received the B.S. and M.S. degrees in communications engineering from National Chiao Tung University, Hsinchu, Taiwan, in 2009 and 2012. Her current research interests include MAC protocol design and LTE-A networks. She has been an engineer targeting on 4G LTE protocol suites since 2012.

Kai-Ten Feng received the B.S. degree from the National Taiwan University, Taipei, Taiwan, in 1992, the M.S. degree from the University of Michigan, Ann Arbor, in 1996, and the Ph.D. degree from the University of California, Berkeley, in 2000. Since August 2011, he has been a full Professor with the Department of Electrical and Computer Engineering, National Chiao Tung University (NCTU), Hsinchu, Taiwan, where he was an Associate Professor and Assistant Professor from August 2007 to July 2011 and from February 2003 to July 2007, respectively. He has also been serving as the Director of EECS International Graduate Program (IGP) at NCTU since February 2014. From July 2009 to March 2010, he was a Visiting Research Fellow with the Department of Electrical and Computer Engineering, University of California at Davis. Between 2000 and 2003, he was an In-Vehicle Development Manager/Senior Technologist with OnStar Corporation, a subsidiary of General Motors Corporation, where he worked on the design of future Telematics platforms and in-vehicle networks. His current research interests include broadband wireless networks, cooperative and cognitive networks, smart phone and embedded system designs, wireless location technologies, and intelligent transportation systems. Dr. Feng received the Best Paper Award from the Spring 2006 IEEE Vehicular Technology Conference, which ranked his paper first among the 615 accepted papers. He also received the Outstanding Youth Electrical Engineer Award in 2007 from the Chinese Institute of Electrical Engineering, and the Distinguished Researcher Award from NCTU in 2008, 2010, and 2011. He has also served on the technical program committees in various international conferences.

Po-Hsuan Tseng received the B.S. and Ph.D. degrees in communication engineering from National Chiao Tung University, Hsinchu, Taiwan, in 2005 and 2011, respectively. Since August 2012, he has been an assistant professor with the Department of Electronic Engineering, National Taipei University of Technology (NTUT), Taipei, Taiwan. From January 2010 to October 2010, he was a visiting researcher with the University of California at Davis. His research interests are in the areas of signal processing for networking and communications, including location estimation and tracking, cooperative localization, and mobile broadband wireless access system design. He is an honorary member of the Phi Tau Phi Scholastic Honor Society of R.O.C.